A Novel Approach to Predict the Unsteady Aerodynamic Behavior of A Delta Wing Undergoing Pitching Motion

N. Sadati[1], M. R. Soltani[2] and A. R. Davari[3]
[1] Professor, Department of Electrical Engineering
[2] Associate Professor, Department of Aerospace Engineering
[3] Ph.D. Student, Department of Aerospace Engineering.
e-mail: sadati@sina.sharif.edu

***Abstract* - In this paper, a new approach based on Generalized Regression Neural Networks (GRNNs) has been proposed to predict the unsteady forces and moments on a 70° swept wing undergoing sinusoidal pitching motion. Extensive wind tunnel testing results were being used for training the network and also for verification of the values predicted by this approach. The Generalized Regression Neural Network (GRNN) has been trained by the aforementioned experimental data and subsequently was used as a prediction tool to determine the unsteady longitudinal coefficient of the pitching delta wing for various reduced frequencies. The obtained results are in a good agreement with those determined by an experimental method.**

I. INTRODUCTION

Many modern fighter aircraft are utilized with highly swept and low aspect ratio wings to improve their supersonic cruise performance. Furthermore, these aircraft are required to have high levels of maneuvering capability and controllability in order to be effective in the combat arena. Among these platforms, delta wings and their combinations are the most common. Their high sweep angle provides favorable drag characteristics at high speed making supersonic flights to be practical. In addition, their sharp leading edges are conducive to flow separation at moderate to high angles of attack, producing substantial non-linear lift known as vortex lift, required during take off, landing, and above all the maneuvers.

Vortex lift is a leading contributor in gaining the tactical advantage desired in a combat environment. The generation of vortex induced lift results in an extension of the maneuvering capability of the fighter aircraft, which in turn requires that both longitudinal and lateral directional stability and control be maintained in this extended angle of attack range. Fig. 1 shows the schematic view of the leading edge vortices on a delta wing. The onset of the leading edge vortices is distinguished by the character of the aerodynamic coefficients, namely by the pronounced non-linearity of the forces and moments with respect to the angle of attack. The size and strength of these vortices increase with increasing the angle of attack, and they become a dominant feature of the flow at moderate to high incidence. Depending on the wing sweep angle, these vortices remain stable through a wide range of angles of attack, up to an angle of 40 degrees for 85 degrees sweep angle [1] and the flow is characteristically steady. Hence they have an important effect on the aerodynamic forces and moments of delta wings.

Theoretical and computational analysis to predict the leading edge vortices and the corresponding aerodynamic forces and moments of delta wings, have already been undertaken by several researchers [2],[3]. The difficulty however appears to be the determination of the position of the vortices and their movement with the angle of attack variation [4].

Unfortunately among the various attempts to simulate the unsteady behavior of the delta wings and predict the corresponding unsteady loads, wind tunnel testing has proven to be the most reliable approach to properly determine the forces and moments. However, this unsteady behavior depends on many variables such as reduced frequency, maximum angle of attack, thickness ratio, leading edge shape, etc. Of course the simulation of all of these parameters in wind tunnel is practically impossible, time consuming and very expensive. Numerical schemes to predict this time dependent behavior, though promising, are not able to give the correct answer yet. In addition, in order to calibrate a numerical code, a huge bank of information are needed that must be supplied either by wind tunnel tests or other means.

Recently, neural networks have been applied to a wide range of aerospace problems. For example, the neural networks have been used in aerodynamic performance optimization of rotor blade

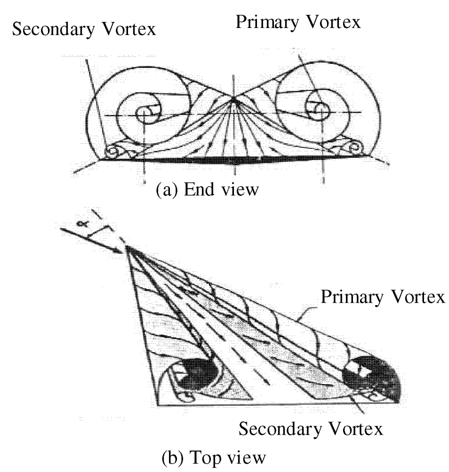

Fig. 1. Schematic of the Vortices on a delta wing.

design [5]. Faller and Schreck [6] have successfully used neural networks to predict the real-time three-dimensional unsteady separated flow fields and aerodynamic coefficients of a pitching wing. It has also been demonstrated that neural networks are capable of predicting measured data with sufficient accuracy to enable identification of instrumentation system degradation [7].

This paper presents the capability of a certain type of neural networks, namely *Generalized Regression Neural Network* (GRNN) to predict the forces and moments on a pitching delta wing in subsonic speeds. Extensive experiments were conducted on a 70-degree swept delta wing undergoing pitching motion with different frequencies. The results have been used to train a GRNN network. The trained network was then used to predict the longitudinal aerodynamic coefficients of the subsonic 70-degree swept delta wing, undergoing sinusoidal pitching motion. The results show remarkable agreement with those obtained by experiments for the same reduced frequencies. The scheme once proved to give the correct results for various conditions, could be used to predict the aerodynamic behavior and is an excellent tool to be used for validating the numerical codes.

II. Flow Field Study Over A Delta Wing

Delta wing vortices contain a great deal of energy, which increases rapidly with angle of attack. This energy induces additional velocity on the upper surface of the wing, reducing the pressure considerably. As a consequence, an additional lift force, known as vortex lift, is generated which increases non-linearly with increasing the angle of attack. This lift increase, up to 50% of the total lift as reported by [1], can be used to improve the takeoff and landing capabilities. These vortices sweep the upper surface flow downward and outboard toward the leading edge. The flow then encounters a steep pressure gradient, which exists between the static pressure under the main vortices and the pressure at the leading edge. As a consequence, the boundary layer separates at the separation line and rolls up into smaller secondary vortices. These secondary vortices have rotational directions, which are opposite to that of the primary vortices. At very high angles of attack, a tertiary vortex underneath the secondary one will form [8], [9]. Fig. 2 shows the growth of the primary vortices with the angle of attack.

Under practical conditions, rapid maneuvering is always required for high performance aircraft. The aerodynamics of dynamic flight maneuvers are more complicated than the static case, mainly due to the unsteady time dependent flow. In dynamic flight maneuvers, the development of the flow field around the wing, fuselage, etc., is a function of alpha, which itself is a function of time. Fast changes of the wing incidence produce large phase lag between the angle of attack and the flow conditions. As a result, the operation of the aircraft may benefit or be hampered by this unsteady flow phenomenon. For many cases, large amplitude harmonic oscillations and large ramp motions have shown beneficial dynamic effects on the flow separation and re-attachment processes.

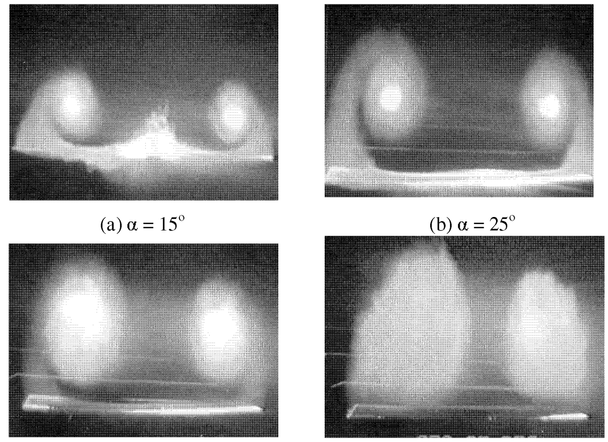

(a) $\alpha = 15^{o}$ (b) $\alpha = 25^{o}$

(c) $\alpha = 30^{o}$ (d) $\alpha = 35^{o}$

Fig. 2. Vortices on a 70^{o} swept wing [15].

Three dimensional unsteady separated flows induced by pitching delta wings, however, are much more complex than their two dimensional counterparts. The dominant feature of delta wing flows, as mentioned previously, is the leading edge vortices, which originate at the wing apex and convert downstream over the wing surface. While for two-dimensional unsteady flows, the onset of the leading edge vortex is associated with the dynamic stall phenomenon. For two-dimensional airfoils the major portion of the lift overshoot obtained in dynamic motion, is attributed to the delay in the flow separation. The lift increment associated with the flow separation and subsequent formation of the leading edge stall vortex, however, is not significant. On the other hand, for delta wings, the flow separation creates a pair of leading edge vortices on the wing suction side. These vortices produce large suction on the wing surface and account for a large portion of the lifting mechanism of the delta wings. Both static and dynamic stalls are initiated by the breakdown of these tightly rolled vortices. While much is known in regard to the flows produced by pitching two-dimensional airfoils and the phenomenology of their dynamic stall, in the case of a delta wing, however, its unsteady aerodynamic properties are practically unknown.

In an oscillatory motion, there exists a different flow structure over the upper surface of the wing between the up and down stroke motions. In upward motion, the burst point reaches the wing apex at a higher angle of attack than it does in the static case and then, in downward motion, the flow remains separated until angles of attack well below the static stall. These differences in the flow pattern create a hysteresis loop, a phenomenon caused by the lag in the flow separation and re-attachment due to the fast variation of the angle of attack [10]. As a result of the hysteresis in the flow structure over the wing surface in oscillatory motion, the values of the aerodynamic force and moments differ between up and down stroke motion. In upward motion, large overshoot in maximum forces and moments and delay in stall angle of attack when compared to the static data is observed. While in downward motion, the dynamic values are substantially less than the static ones. Thus in an oscillatory motion, forces and moments lag the instantaneous angle of attack, owing to the time lag in the flow structure. The magnitude of the overshoots and the size of the hysteresis loops are a strong function of the reduced frequency. Taking advantage of this, the performance of a fighter aircraft in the combat arena can be greatly enhanced.

III. GENERALIZED REGRESSION NEURAL NETWORKS (GRNNS)

The neural networks in general have two main components; the processing elements called neurons or nodes and the connection between the nodes, each having its own weight. The neurons are the information processors and the connection functions are the information storage. Each processing element first calculates a weighted sum of the input signals and then applies a transfer function called the activation function, such as a tangent hyperbolic or the sigmoid function to the weighted sum, and outputs the result [11]. The neurons within the network are arranged in an input layer, one or more hidden or processing layers and an output layer. In a prediction problem such as aerodynamic modelling, the number of neurons in the input layer is equal to the number of input variables, and also the number of neurons in the output layer equals the number of predicted variables. Selection of the rest of the architecture of the network in terms of the number of neurons in the hidden layer, the learning rate and etc., is not an exact science and one has to resort to trial and error methods to find a suitable network structure for a given problem.

The General Regression Neural Network (GRNN) was first introduced by Donald Specht in 1991 [12] to perform a general regression. A basic GRNN network is shown Fig. 3.

Considering the vectors X and Y, in system identification, the dependent variables Y and X could be considered as system's output and input, respectively. The regression of a dependent variable Y on an independent variable X is the computation of the most probable value of Y for each value of X by taking a finite number of X measurements, taking the associated Y values into account. For this reason, it is usually necessary to assume some functions with unknown parameter a_i. The values of the parameters are chosen to provide the best fit to the measured data. It should be noted that the approach

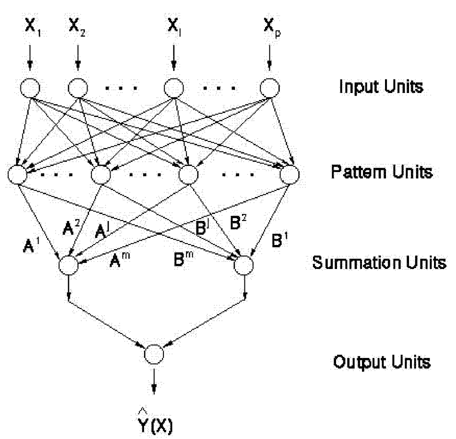

Fig. 3. The Generalized Regression Neural Network (GRNN).

functional form. It allows the appropriate form to be expressed as a probability density function (PDF) that is determined empirically from the observed data. Thus the approach is not limited and does not require any pre-knowledge of any particular form.

Assume that the $f(x,y)$ represents the known joint continuous PDF of the vector random variable x and a scalar random variable y. Let X be the particular measured value of the random variable x. The conditional mean of y for given X (also called the regression of y on X) is given by

$$E(y|X) = \frac{\int_{-\infty}^{\infty} y\, f(X,y)\, dy}{\int_{-\infty}^{\infty} f(X,y)\, dy} \tag{1}$$

When the density function $f(x, y)$ is not known, it is usually estimated from a sample of observations of x and y. For a non-parametric estimate of $f(x,y)$, Prazen [13] proposed the class of consistent estimators for one dimensional cases. Further estimators for multidimensional cases were proposed by Cacoullos [14]. These estimators are good choices for estimating the probability density function f, if it can be assumed that the density is continuous and the first partial derivatives of the function evaluated at any x are small. The probability estimator $\hat{f}(X,Y)$ is based on sample values X^i and Y^i of the random variables x and y, respectively.

$$\hat{f}(X,Y) = \frac{1}{(2\pi)^{(p-1)/2}\sigma^{(p+1)}} \cdot \frac{1}{n} \sum_{i=1}^{n} \exp\left[-\frac{(X-X^i)^T(X-X^i)}{2\sigma^2}\right] \exp\left[-\frac{(Y-Y^i)^2}{2\sigma^2}\right] \tag{2}$$

where n is the number of sample observations and p is the dimension of the vector variable x. Interchanging the order of integration and summation, after some simplifications, the desired conditional mean indicated by $\hat{Y}(X)$, will be determined as

$$\hat{Y}(X) = \frac{\sum_{i=1}^{n} Y^i \exp(-\frac{D_i^2}{2\sigma^2})}{\sum_{i=1}^{n} \exp(-\frac{D_i^2}{2\sigma^2})} \tag{3}$$

where the scalar function D_i^2 is defined as $D_i^2 = (X-X^i)^T(X-X^i)$.

Peazen and Cacoullos have shown that these form of estimators are consistent estimators, which means that their ability to converge to underlying probability density function $f(x,y)$, at all points (x, y), where the density function is continuous and $\sigma = \sigma(n)$ is a decreasing function of n, such that $\lim_{n\to\infty} \sigma(n) = 0$ and $\lim_{n\to\infty} n\sigma^n(n) = \infty$. However it should be noted that σ is one of the most important parameters in an GRNN network. The best value for σ is actually the one which increases the network generalization capability to its maximum value. Suppose that a network has been trained with m series of patterns (X^i, Y^i). It is desired to get an optimum value for σ to minimize the mean error. In other words, if k patterns $(X^i,$

$Y^i)_{i=1,\dots,k}$ are used to check the generalization capability of the network, an optimum σ minimizes the following expression

$$E_{mean} = \frac{\sum_{i=1}^{k} \left| Y_e(X^i) - Y^i \right|}{k} \tag{4}$$

This k set of input patterns could be a combination of m teacher data set and some new input/output data, or a set containing some random patterns or a new set of patterns different from the initial ones used as teacher data. However for all of the above cases, the optimum value for σ can be obtained easily by trying some values for σ and calculating the mean errors in the output results. The optimum σ corresponds to the minimum value of these errors.

In the present investigation, a 70^o swept delta wing undergoing sinusoidal pitching motion in subsonic flow was considered. Several experiments at different conditions have been carried out. The values of the pitching frequency, angle of attack and Reynolds number for some experimental cases were used as teaching data to train the network. The system outputs were normal force, drag and the pitching moment coefficients (C_N, C_D and C_m), which have been already obtained from the experiments. Now to check the ability of this network, further experiments in new conditions have been conducted and the network was used to predict the normal force, drag and pitching moments for theses new input data. The network outputs then were compared with those of experimentally measured values. The results show remarkable agreement between the experiments and GRNN outputs.

IV. Experimental Procedure

All experiments were conducted in the subsonic wind tunnel of The Ohio State University, as stated in [15]. It is an in draft, open circuit tunnel which exhausts to the atmosphere. It has a test section of approximately five feet wide, three feet high, and 8 feet long, and operates at speeds from zero to 220 ft/sec at Reynolds number of up to 1.3×10^6 per foot. The model used to perform these experiments was a simple flat plate delta wing of 70^o leading edge sweep, a 15-inch span at the trailing edge and a thickness ratio of 0.012. The wing was constructed of aluminium.

A system was designed which pitched the models through large amplitude oscillations. The oscillation system uses a belt and pulley arrangement to reduce the motor R.P.M. to speeds from zero to 2.3 hertz. A computer program was written which would design a cam to produce the desired motion. The equation for the sinusoidal motion with amplitude of 55 degrees were input to the program. The resulting cam produced a sinusoidal oscillation of the model inside the tunnel during the pitching motion.

The 70-degree aluminium delta wing model was sinusoidal oscillated in pitch from 0 to 55 degrees angle of attack at reduced frequencies from 0.015 to 0.089 and at a Reynolds number of 1.43×10^6. Data for each cycle were taken at a frequency of 100-1000 Hz and up to 1000 data points were collected.

V. Results and Discussion

Figs. 4a through 4d show the dynamic variation of the normal force coefficient with the angle of attack for one oscillation cycle for the reduced frequencies of k = 0.015, 0.020, 0.034 and 0.045. Substantial maximum force overshoot, a delay in stall angle of attack and large hysteresis between increasing and decreasing angle of attack are seen for even the smallest frequency tested. During the pitch up motion, the lag in the leading edge vortex system and its breakdown development resulted in higher forces and moments at moderate to high angles of attack. While in the pitch down motion, the flow remained separated until the angles of attack well below the static stall, creating a hysteresis loop [16]. As it can be seen, the experimental data and those predicted by the GRNN method are in a good agreement. As shown in Fig. 4, for all frequencies, the linear region of the curve is exactly predicted by the GRNN. However after the maximum value of the normal force coefficient, where the slope reverses its sign, some tolerable discrepancies can be seen in the predicted values. The data for all frequencies show that when there is an abrupt change in the slope, some deviations will be seen in the predicted values by the GRNN. However the error, as seen in Fig. 4, is sufficiently small.

Fig. 5 shows the effect of reduced frequency on the drag coefficient of the model undergoing large amplitude sinusoidal oscillations. Reduced frequency has a pronounced effect on the maximum value of the drag coefficient, the angle of attack at which it occurs and also the shape of the hysteresis loop between the upstroke and down stroke values of the drag coefficients. These variations are probably due to the normal force coefficient during oscillations. Again it can be seen that the GRNN method has predicted the drag coefficient exactly except for the regions in the curve where a sudden change in the slope has occurred.

Fig. 6 shows the impact of the large amplitude sinusoidal pitching motion for different reduced frequencies on the model pitching moment. The influence of pitch rate on the character of the pitching moment hysteresis loop and its magnitude is apparent. In the pitch up motion, increasing the reduced frequency, delays the deterioration of the leading edge vortices to higher angles of attack, thus producing higher negative pitching moment. During the pitch down motion, the persistence of the separated flow, delays the re-attachment process of the vortices to lower angles of attack, producing higher nose up pitching moment that has considerable impact on the width of the hysteresis loop. The values of the moments predicted by GRNN confirm the results and show this loop. Again some tolerable discrepancies can be seen in the regions where the slope changes dramatically.

As mentioned before, it is so important to choose the optimum value of σ in an GRNN network. Changes in this parameter can alter the results significantly. Fig. 7 shows the sensitivity of the predicted values of the aerodynamic coefficients to σ. As it is shown, only the optimum value of this parameter gives the best prediction and other values will result in a wrong prediction.

Fig. 8 shows the effects of the reduced frequency on longitudinal aerodynamic behavior of a 70^{o} delta wing undergoing sinusoidal pitching motion as predicted by the aforementioned trained neural network. According to this figure, the hysterises loop will be wider as the reduced frequency increases. As a result, the difference between the up stroke and down stroke aerodynamic behavior will be increased.

VI. CONCLUSION

A new approach based on Generalized Regression Neural Networks (GRNNs) has been introduced to predict the unsteady forces and moments on a pitching delta wing. Extensive wind tunnel testing results were used to train the network and verify the predicted values. The results show an acceptable agreement between the experimental results and those predicted by GRNN. The present approach shows the ability of the neural networks in predicting the unsteady aerodynamic behavior of delta wings. This method can greatly reduce the number of wind tunnel tests needed to investigate the unsteady aerodynamic phenomena occur on these kind of wings. Although several numerical software have been developed to predict these phenomena, the neural network based methods seem to have better performance from time and cost points of view.

GRNN accurately predicts the unsteady loops of normal force, drag and pitching moment for a pitching slender delta wing. However, it should be noted that in a hysteresis loop, there are some points where the curve slope changes abruptly and in these regions, the results obtained by GRNN show some discrepancies in compare with those obtained using experimental data. Also as it is shown by the GRNN and confirmed by the experiments, there is a large overshoot in the dynamic loads for all reduced frequencies. Dynamic stall angle also increases with increasing the reduced frequency.

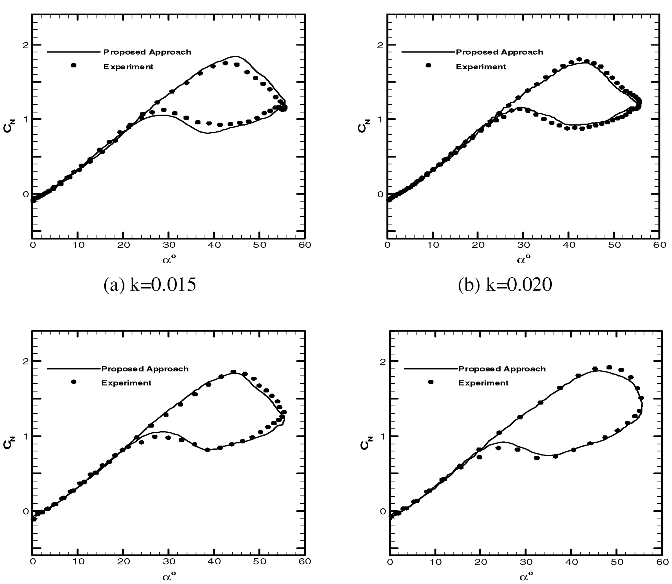

(a) k=0.015 (b) k=0.020

(c) k=0.024 (d) k=0.045

Fig. 4. Variations of normal force coefficient with α.

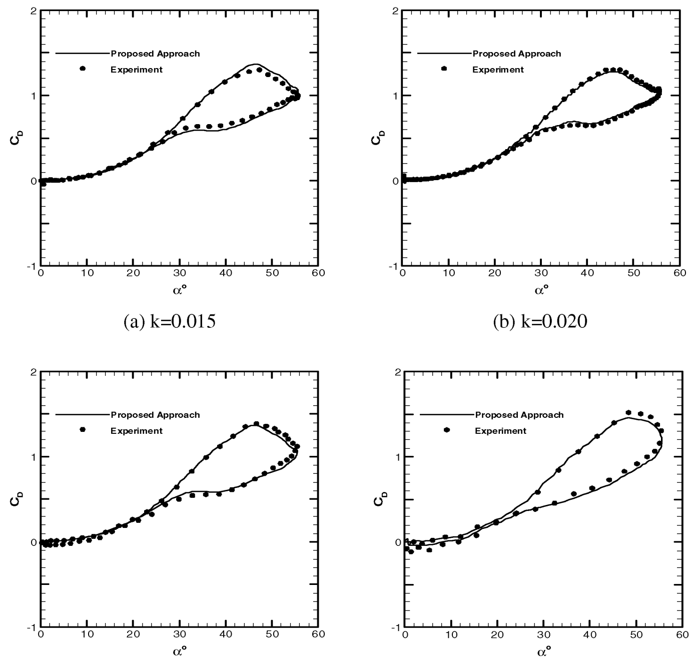

(a) k=0.015 (b) k=0.020

(c) k=0.024 (d) k=0.045

Fig. 5. Variations of drag coefficient with α.

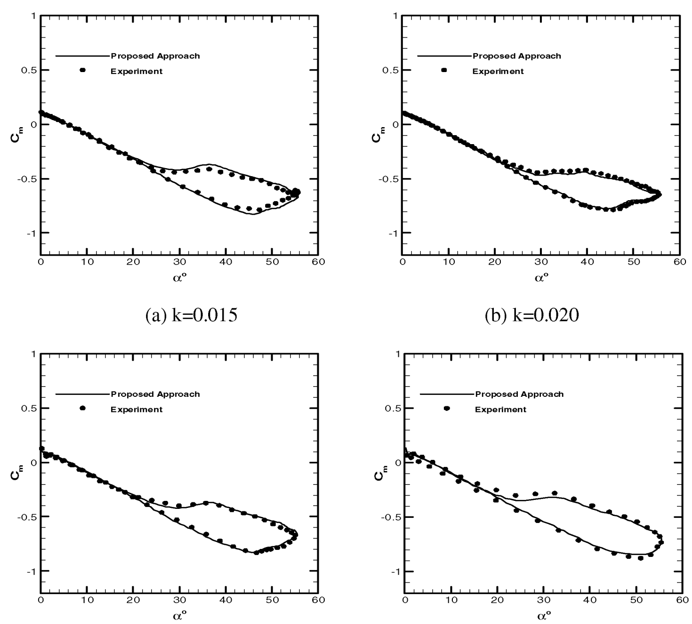

(a) k=0.015 (b) k=0.020

(c) k=0.024 (d) k=0.045

Fig. 6. Variations of the pitching moment coefficient with α.

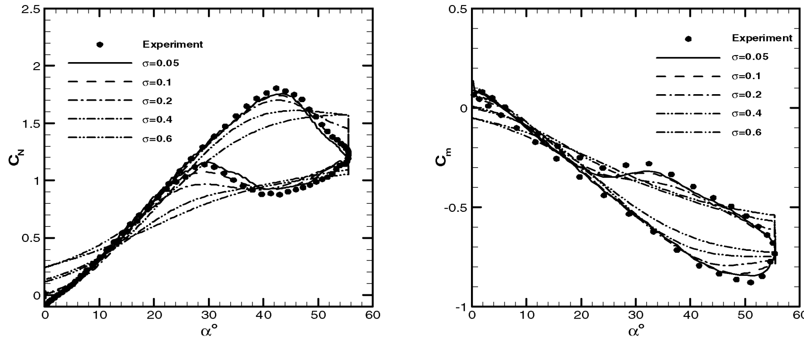

(a) Prediction of C_N (b) Prediction of C_m

Fig. 7. Effectsof σ on the prediction accuracy.

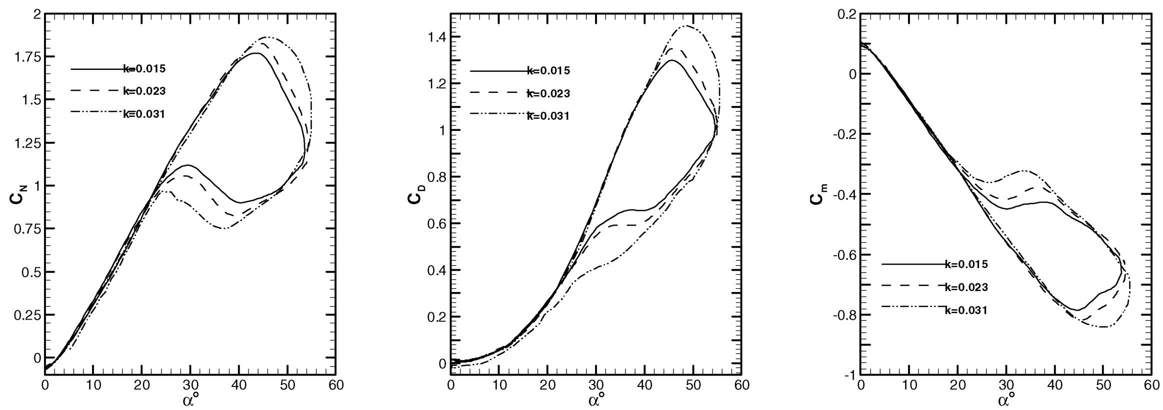

(a) Normal force coefficient (b) Drag coefficient (c) Pitching moment coefficient

Fig. 8. Effects of reduced frequency on the aerodynamic coefficients, predicted by the proposed approach.

.

REFERENCES

[1] W.H. Wentz and D.L. Kohlman, “Vortex breakdown on slender sharp edged wings,” AIAA Paper, pp. 69-778, 1969.

[2] J. M. Walker, H. E. Helin and J. H. Strickland, “An experimental investigation of an airfoil undergoing large-amplitude pitching motions,” AIAA Journal, vol. 23, no. 8, Aug. 1985.

[3] J. F. McKernan, F. M. Payne and R. C. Nelson, “Vortex breakdown measurements on a 70 deg. sweep back delta wing,” Journal of Aircraft, vol. 25, no. 11, Nov. 1988.

[4] L. E. Ericsson, “Vortex unsteadiness on slender bodies at high incidence,” Journal of Spacecraft and Rockets, vol. 24, no. 4, July 1987.

[5] W.J. LaMArsh, J.L. Walsh and J.L. Rogers, “Aerodynamic performance optimization of a rotor blade using a neural network as the analysis,” AIAA Paper, pp. 92-4837, Sept. 1992.

[6] W.E. Faller and S.J. Schreck, “Real time prediction of unsteady aerodynamics: application of aircraft control and maneuverability enhancement,” IEEE Trans. on Neural Networks, vol. 6, no. 6, 1995.

[7] R.L. McMiller, J.E. Steck and K. Roshaz, “Appliction of an artificial neural network as a flight test data estimator,” Journal of Aircraft, vol. 32, no. 5, 1995.

[8] J.K. Harvey, “Some measurements on a yawed slender delta wing with leading edge separation,” Aeronautical Research Council, Reports and Memoranda no. 3160, Oct. 1958.

[9] M. Menke and I. Gursul, “Nonlinear response of vortex breakdown over a pitching delta wing,” Journal of Aircraft, vol. 36, no. 3, 1999.

[10] M.R. Soltani, S.A. Ebrahimi and A.R. Davari, “A simple analytical method for predicting the amplitude and frequency of a delta wing model undergoing rocking motion,” AIAA Paper, pp. 2002-0710, March 2002.

[11] S.Y. Kung, Digital Neural Network. Prentice-Hall Inc., 1993.

[12] D.F. Specht, “A general regression neural network,” IEEE Trans. on Neural Networks, vol.2, no. 6, pp. 568-576, 1991.

[13] F. Parzen, “On estimation of a probability density function and mode,” Ann. Math. Statist., vol 33, pp. 1065-1076, 1962.

[14] T. Cacoullos, “Estimation of a multivariable density,” Ann. Math. Statist., vol. 18, no. 2, pp. 179-189, 1966.

[15] M.R. Soltani, An Experimental Study of the Relationship Between Forces and Moments and Vortex Breakdown on A Pitching Delta Wing. Ph.D. Thesis, Department of Aeronautical Engineering, University of Illinois at Urbana-Champaign,1992.

[16] B.A. Broeren and M.B. Bragg, “Flow field measurements over an airfoil during natural frequency oscillations near stall,” AIAA Journal, vol. 36, no. 5, 2001.